Virology 525 (2018) 96–105

Contents lists available at ScienceDirect

Virology

journal homepage: www.elsevier.com/locate/virology

Rotavirus RNAs sponge host cell RNA binding proteins and interfere with their subcellular localization

Alfonso Oceguera, Andrea V. Peralta[1], Gustavo Martínez-Delgado[2], Carlos F. Arias, Susana López*

Departamento de Genética del Desarrollo y Fisiología Molecular, Instituto de Biotecnología, Universidad Nacional Autónoma de México, Cuernavaca, Morelos 62210, Mexico

ARTICLE INFO

Keywords:
Rotavirus
Virus host cell interactions
RNA granules
RNA sponges
RNA binding proteins
P-bodies
GW-bodies

ABSTRACT

Cellular mRNAs cycle between translating and non-translating pools, polysomes compose the translating pool, while RNA granules contain translationally-silenced mRNAs, where the RNAs are either stored in stress granules, or accumulate in processing bodies (PBs) or GW-bodies, which have an important role in RNA degradation. Viruses have developed measures to prevent the deleterious effects of these structures during their replication. Rotavirus, the most common agent of viral gastroenteritis, is capable of establishing a successful infection by counteracting several of the antiviral responses of its host. Here, we describe that in rotavirus-infected cells the distribution of several RNA binding proteins is changed causing the disaggregation of PBs, the relocalization of GW-body proteins, and the cytoplasmic accumulation of HuR, a predominantly nuclear protein. We show that this redistribution of proteins is more likely caused by the accumulation of viral RNA in the cytoplasm of infected-cells, where it might be acting as an RBP sponge.

1. Introduction

Rotaviruses are one of the main causes of acute, severe, life-threatening gastroenteritis in children around the world causing an estimate of 220,000 deaths annually, mainly in low-income countries, despite the fact that a successful vaccination program against these viruses began in 2006 (Crawford et al., 2017). This underscores the importance of studies aimed to further characterize the replication cycle of rotavirus looking for ways to control or to decrease its replication.

The rotavirus mature particle is formed by a triple layer of proteins that surrounds the genome formed by 11 segments of double stranded RNA (dsRNA). The inner layer is formed by VP2 and within this layer there are two viral enzymes in very low amounts, VP1 the virus RNA-dependent RNA polymerase (RdRp), and VP3, the guanylyl-methyltransferase and phosphodiesterase of the virus. The middle layer is formed by VP6, which is surrounded by the outer most layer composed of VP4 and VP7. After entering susceptible cells, the outer layer proteins are released and the double layer capsid becomes transcriptionally active, giving rise to 11 mRNAs that direct the synthesis of the viral proteins and also serve as templates for the synthesis of the genomic dsRNA (Estes, 2013). The transcription activity of the viral particle is extremely efficient, and in infected cells there can be around 300,000 copies per cell of one of the smallest transcripts (Rubio et al., 2013).

As any other virus, rotaviruses have developed strategies to dodge the antiviral responses of the host cell. These viruses take over the translation machinery of the cell, so that by eight hours post-infection most of the translation apparatus is committed to translate viral mRNAs. Also, during the infection rotavirus prevents the formation of stress granules (SG), which are dynamic cytoplasmic aggregates of stalled preinitiation complexes that are formed during different types of cell-stress and that arrest the translation of most mRNAs (Rubio et al., 2013). SGs form part of a growing group of RNA granules, aggregates of different RNAs and proteins that have been recently characterized (Tsai and Lloyd, 2014). Processing bodies, or PBs, are the second largest group of cytoplasmic aggregates; in contrast with SGs, these structures are constitutively present in the cell cytoplasm and are enriched in components of the 5'-3' mRNA decay machinery, including deadenylases, decapping enzymes, and exonucleases, and thus PBs are thought to be places where RNA is degraded. GW182 bodies (GW-bodies) represent another group of recently described RNA granules that in addition to the proteins found in PBs, also contain a group of RNA binding proteins (RBPs) involved in nonsense-mediated decay and

* Correspondence to: Instituto de Biotecnología, Universidad Nacional Autónoma de México, Avenida Universidad 2001, Colonia Chamilpa, Cuernavaca, Morelos 62210, Mexico.
E-mail address: susana@ibt.unam.mx (S. López).
[1] Present address: Consejo Nacional de Investigaciones Científicas y Tecnológicas (CONICET), Godoy Cruz 2290, C1425FQB Buenos Aires, Argentina.
[2] Present address: Instituto Cumbres Lomas, Mexico City, Mexico.

https://doi.org/10.1016/j.virol.2018.09.013
Received 29 May 2018; Received in revised form 13 September 2018; Accepted 17 September 2018

microRNA-mediated silencing, such as GW182 and Ago proteins. It has been recently proposed that PBs and GW-bodies represent two separate pools of sequestered non-translating mRNAs (Patel et al., 2016).

It has been reported that, in addition to preventing the formation of SGs, in rotavirus-infected cells the formation of SGs is inhibited even when cells are induced to form these structures by treatment with arsenite, a classic SG inducer (Montero et al., 2008); however, the mechanism by which the formation of SGs is prevented during the infection has not been determined. More recently, Bhowmick et al. (Bhowmick et al., 2015) found that different rotavirus strains were able to inhibit, or decrease, the formation of PBs during the infection. They reported that the deadenylating Pan3 enzyme was sent to degradation, while the exonuclease Xrn1 and the decapping enzyme Dcp1 were relocalized from the cytoplasm to the nucleus, and it was also shown that these three PB-components were able to interact, directly or indirectly, with viral RNA (Bhowmick et al., 2015). The molecular mechanisms by which these proteins were relocalized to the nucleus were not established.

The distribution of mRNAs between polysomes, SGs, and PBs in a given cell condition determines the rate of mRNA translation and degradation, thus directly influencing gene expression (Anderson and Kedersha, 2008). When an mRNA is targeted for degradation in the cytoplasm, its polyA tail is initially removed, and then it is subjected to exonucleolytic degradation either in the 3′ to 5′direction by the exosome, or it is marked by the LSM1–7 complex for decapping by Dcpn1/2, and degraded by Xrn1 in the 5′ to 3′ direction. Many of the cellular proteins involved in these processes are aggregated in PBs or in GW-bodies (reviewed in Moon and Wilusz (2013)). Since RNA granules have fundamental roles in the fate of cellular and viral mRNAs, several viruses have developed measures to prevent the deleterious effect of these structures during their replicative cycles (reviewed in Tsai and Lloyd (2014)). Here, we decided to determine whether rotaviruses have developed a strategy to prevent the antiviral effects of the RNA granules. We found that during rotavirus infection the distribution of several RBPs is changed, causing the disaggregation of PBs, the relocalization of proteins constituent of GW-bodies, and the cytoplasmic accumulation of HuR, an RBP that is predominantly nuclear. We also demonstrate that the redistribution of host cell proteins is more likely caused by the accumulation of viral RNA in the cytoplasm of infected cells, where it might be acting as a sponge for several host RNA binding proteins.

2. Results

2.1. Rotavirus infection decreases the amount of Dcp1- and Xrn1-stained PBs

To determine if there was an alteration in the distribution or amount of PBs during rotavirus infection, we compared by immunofluorescence the presence of these RNA granules in mock-infected or rotavirus-infected cells, using antibodies against two of the most common PBs markers: Dcp1 and Xrn1; as a marker of infection, we used antibodies against rotavirus NSP2, which is a non-structural protein that forms part of the viroplasms (Fig. 1). We found that there was a nice, even distribution of small puncta characteristic of PBs when mock-infected MA104 cells were stained with antibodies to Dcp1 or to Xrn1. This distribution changed in cells that were infected with rotavirus, where there was an apparent decrease in the number of PBs. To analyze quantitatively the change in the number of PBs stained by Dcp1 and Xrn1 antibodies, we determined the number of PBs per cell present at different times post-infection. Fig. 1B shows that the number of PBs decreased as the infection proceeded reaching a decrease of 77% and 74% for Dcp1 and Xrn1, respectively, at 8hpi. To determine if the reduction in the number of PBs observed in rotavirus-infected cells was due to a reduction in the amount of Xrn1 and Dcp1 proteins, or to a redistribution of these proteins in the cell, we quantitated the amount of Xrn1 and Dcp1 proteins present in cells at different times post-infection and compared them with mock-infected cells by western blot assays, using specific antibodies against these two proteins (Fig. 1C). We found that there were no significant changes in the levels of Dcp1 and Xrn1, indicating that the reduction in the number of PBs observed is not due to a decrease in the amount of these proteins but more likely to a redistribution of these proteins caused by the infection.

2.2. The number of PBs present in infected cells is affected by the amount of viral RNA

Since the amount of Dcp1 and Xrn1 proteins did not change in the course of rotavirus infection, but the number of PBs decreased, it was possible that these PB proteins were no longer aggregated in RNA granules, but homogeneously dispersed in the cell cytoplasm. We have established that during rotavirus infection the amount of viral transcripts is very high (at 8 hpi there are about 300,000 copies of the NSP4 transcript per cell) (Rubio et al., 2013), thus we reasoned that a plausible explanation for the disaggregation of PBs could be that during the infection, some of the proteins that formed part of these RNA granules became associated with viral RNAs. To test this idea, we silenced the expression of VP1 (the viral RdRp) or VP3 (the guanylyl-methyl transferase) in rotavirus-infected cells and looked for the number of PBs present in these cells. We have previously reported that silencing the expression of these two viral genes by RNA interference resulted in a decrease of about 90% of the viral mRNAs and genomic dsRNA, while the synthesis of the viral proteins was not affected (Ayala-Breton et al., 2009). As a control, we also silenced the expression of NSP3, which results in an increase of viral mRNA and dsRNA levels of about three times (Montero et al., 2006). The level of silencing of each of the viral proteins was tested by western blot using specific antibodies (Fig. 2A), the effect on viral RNA synthesis was determined by quantitative RT-PCR assay (Ayala-Breton et al., 2009) (Fig. 2B), and the number of PBs stained with antibodies to Xrn1 or Dcp1 was counted in siRNA-treated cells that had been infected or not with rotavirus (Fig. 2C and D). We found that, while in cells transfected with an irrelevant siRNA the number of Dcp1- and Xrn1-stained PBs represented about 30% the number of PBs observed in mock-infected cells, when either VP1 or VP3 were silenced the number of these RNA granules increased twice or more (Figs. 2C and 2D); accordingly, the amount of viral RNA detected was reduced by 80–90% that of the control transfected cells (Fig. 2B). Interestingly, when NSP3 was silenced and the amount of viral RNA increased in the cytoplasm, the number of PBs was equal or slightly less to that obtained in control cells treated with the control siRNA. Together, these results suggest that the amount of viral RNA present in the cytoplasm of infected cells affects the aggregation of Dcp1 and Xrn1 into RNA granules, and might explain the reduction in the number of PBs observed in infected cells.

2.3. GW182 and Argonaute 2 change their localization during rotavirus infection

As previously mentioned, it has been shown that besides PBs, a different kind of RNA granules named GW-bodies could be present in the cell´s cytoplasm (Patel et al., 2016). To determine if GW-bodies were present in MA104 cells and if their distribution and/or number were also altered during rotavirus infection, we looked for these structures by immunofluorescence using antibodies to GW182 and to Argonaute 2 (Ago2) protein, which is a component of the RISC machinery and has been found in SGs, PBs, and GW-bodies (Poblete-Duran et al., 2016) (Fig. 3). In this case, we found that in mock infected cells the distribution of both proteins was in a punctuated pattern throughout the cytoplasm; the signal observed with the antibody to GW182 was similar to that observed with Dcp1 and Xrn1 antibodies, in which a discrete amount of small granules in each cell could be observed. In contrast, with the antibody to Ago2 we observed an increased number of small foci, which might represent the different RNA granules

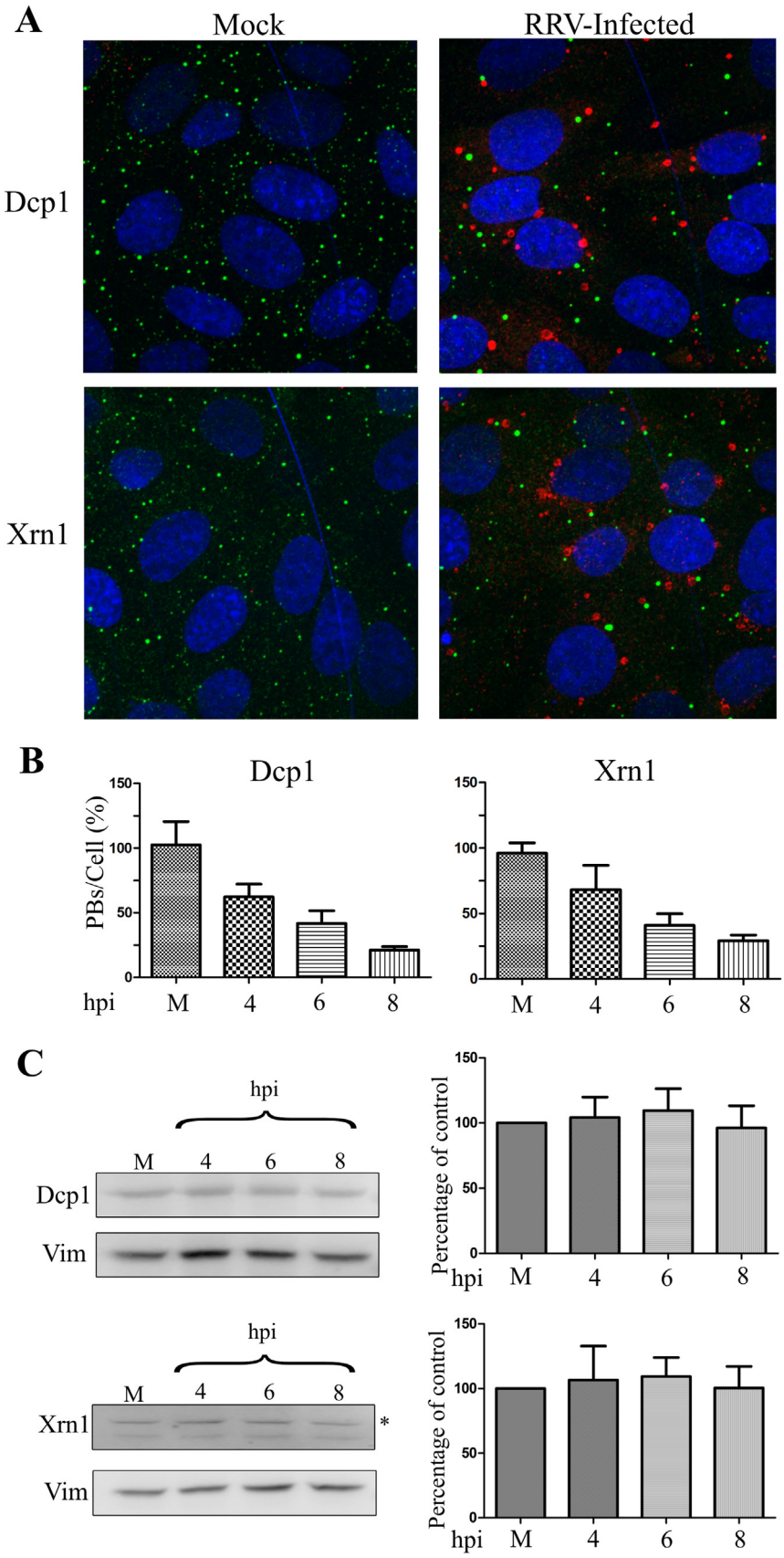

Fig. 1. The amount of PBs decreases during rotavirus infection. A) Confluent MA104 cells grown in coverslips were mock-infected or infected with RRV at an MOI of 5, and 8 hpi cells were fixed and stained with antibodies against Dcp1, or Xrn1 (green), or to NSP2 (red) as indicated under Section 4. The cell nuclei were stained with 4,6-diamidino-2-phenylindole (DAPI; in blue). B) Confluent MA104 cells grown in coverslips were mock-infected or infected with RRV at an MOI of 5, and at the indicated times post infection (hpi), cells were fixed and stained as indicated in A) and the number of PBs was counted by a macro made from image J applications for image analysis. Data shown were obtained by counting 300 cells in each condition. Values are expressed as the percentage of the number of PBs counted in uninfected cells which were, on average, 12 PBs/cell. The arithmetic mean ± SEM of three independent experiments is shown. **D)** MA104 cells were mock-infected or infected with RRV at an MOI of 5 and at the indicated times cells were lysed and the proteins were resolved in an SDS-10% PAGE, transferred to nitrocellulose and Dcp1 or Xrn1 were detected by immunoblot analysis with the indicated antibodies. Left, representative western blots stained with anti-Dcp1 or anti-Xrn1. Vimentin (Vim) was used as a loading control; the asterisk indicates the band that corresponds to Xrn1. Right, quantitation of the amount of protein detected under each condition. The relative amount of the indicated protein was calculated by densitometry of the bands using ImageQuan TL software (Amersham, Biosciences). Values represent the amount of protein detected as a percentage of the amount of protein detected in mock-infected cells normalized with its corresponding loading control (Vim). The arithmetic mean ± SEM of three independent experiments is shown.

to which this protein is associated. In rotavirus-infected cells we found that the localization of these two proteins behaved differently, in the case of GW182, the number of GW-bodies increased, and apparently a portion of this protein co-localized with viroplasms, while in the case of Ago2 most of the puncta stained with the antibody became perinuclear and appear to accumulate around viroplasms (Fig. 3). These

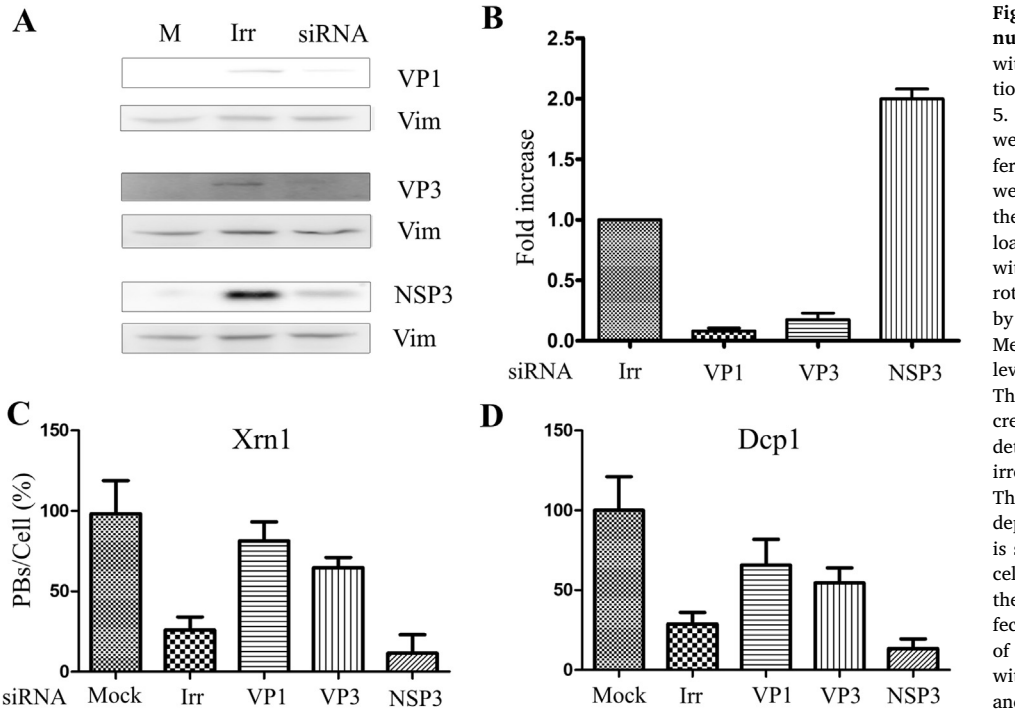

Fig. 2. The level of viral RNA affects the number PBs. A) MA104 cells were transfected with the indicated siRNAs, 72 h post-transfection cells were infected with RRV at an MOI of 5. Eight hpi cells were lysed and the proteins were resolved in an SDS-10% PAGE, transferred to nitrocellulose and VP1, VP2, or NSP3, were detected by immunoblot analysis using the indicated antibodies, or Vimentin (Vim) as loading control. B) Cell lysates were extracted with Trizol and the RNA of gene segment 10 of rotavirus, and the 18S rRNA were quantitated by RT-qPCR as indicated under Materials and Methods. The results were normalized to the levels of 18S rRNA detected in each sample. The RT-qPCR results are expressed as fold increase relative to the amount of gene 10 RNA detected in cells that were transfected with the irrelevant siRNA (Irr), which was taken as 1. The arithmetic mean ± SEM of three independent experiments performed in triplicate is shown. C) and D) In parallel wells, MA104 cells grown in coverslips were transfected with the indicated siRNAs, 72 h hours post-transfection cells were infected with RRV at an MOI of 5, and 8 hpi cells were fixed and stained with antibodies against Xrn1 (C), or Dcp1 (D), and the number of PBs was counted as indicated in Fig. 1. Data shown were obtained from counting 300 nuclei in each condition. Values are expressed as percentage of the number of PBs counted in uninfected nuclei (M), which were on average 12 PBs/nuclei. The arithmetic mean ± SEM of three independent experiments is shown.

observations suggest that the PBs stained with Dcp1 and Xrn1 antibodies are different from the granules stained with GW182 and Ago2.

To establish whether the relocalization observed for GW182 and Ago2 proteins was also driven by the amount of viral RNA present in the cytoplasm of infected cells, we used the same strategy described above to reduce the amount of viral RNA in the infection by silencing the expression of either VP1 or VP3, and looked for the distribution of these proteins in silenced and infected cells by immunofluorescence microscopy (Fig. 4). Rotavirus-infected cells treated with an irrelevant siRNA showed the same distribution of GW182 and Ago2 proteins as that observed in the infected cells that were not treated with siRNAs; however, when either VP1 or VP3 were silenced, the distribution of these two proteins changed; GW182 no longer colocalized with viroplasms, and its distribution appeared almost identical to that observed

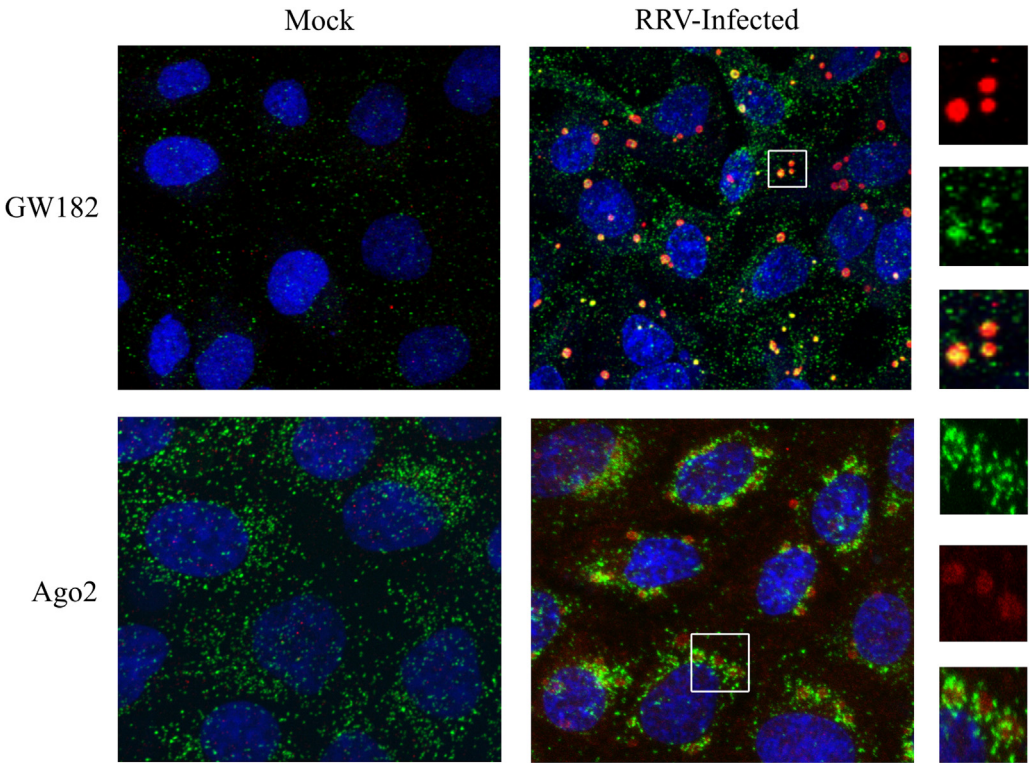

Fig. 3. GW182 and Argonaute 2 change their distribution in rotavirus-infected cells. Confluent MA104 cells grown in coverslips were mock-infected or infected with RRV at an MOI of 5, and at 8 hpi cells were fixed and stained with antibodies against GW182, or Ago2 (green), and to NSP2 (red); cell nuclei were stained with DAPI (blue) as indicated under Section 4. The images for GW182 staining were acquired in an Olympus confocal FluoView 1000 multifotonic microscope, and for Ago2 staining a 3I Marianas spinning disk confocal microscope was used.

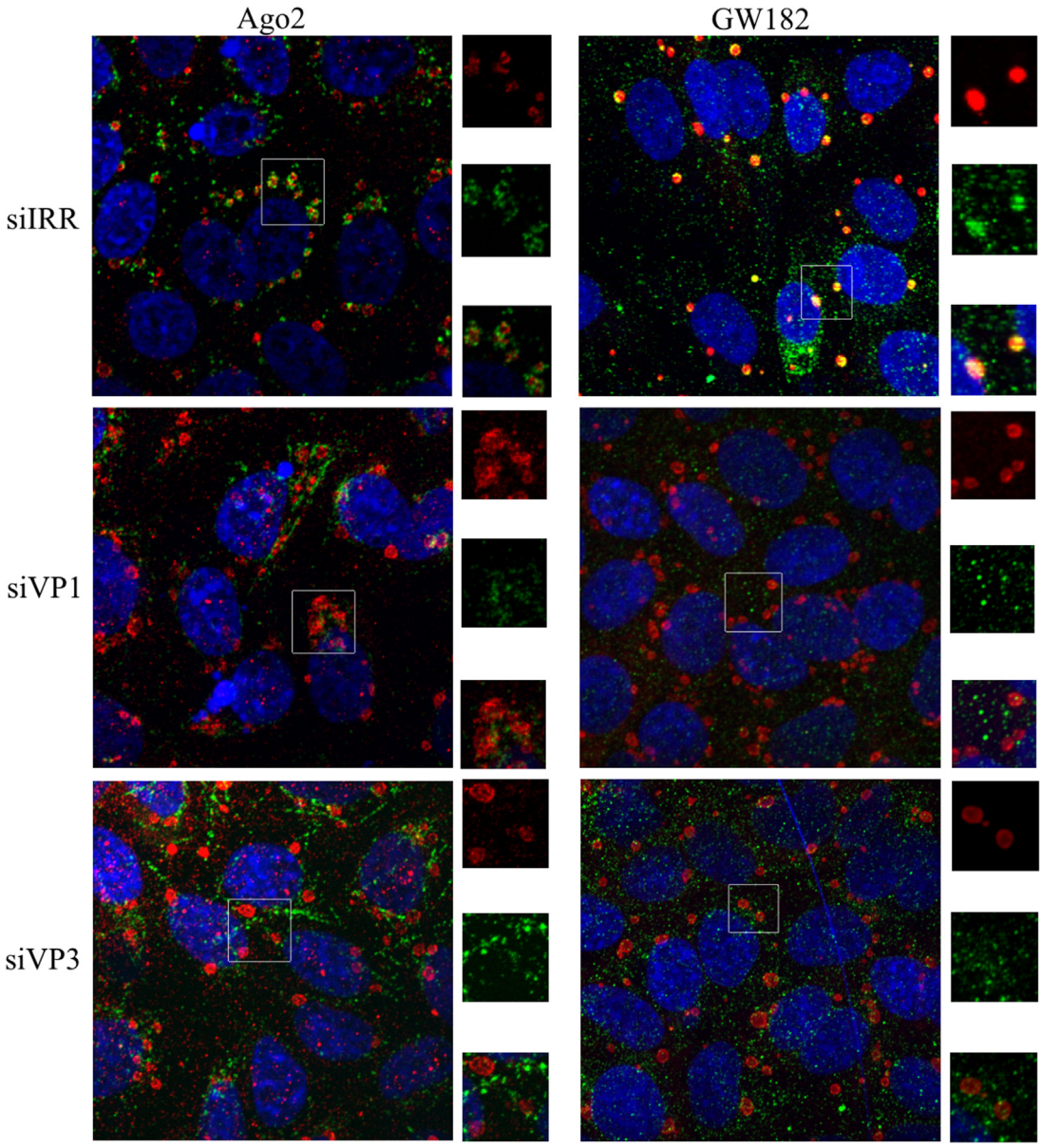

Fig. 4. The distribution of GW182 and Ago2 during rotavirus infection depends on the amount of viral RNA. MA104 cells grown in coverslips were transfected with the indicated siRNAs; seventy-two hours post-transfection cells were infected with RRV at an MOI of 5, and at 8 hpi cells were fixed and stained with antibodies against GW182, or Ago2 (green), and to NSP2 (red) as indicated under Section 4. Cell nuclei were stained with DAPI (blue). The images were acquired in a 3I Marianas spinning disk confocal microscope. Representative colocalization images of NSP2 with Ago 2 and GW182 are shown. Manders' correlation coefficients (M ± SE), were obtained analyzing 12 cells per condition as indicated under Materials and Methods, and are as follows: Ago2-siIrr (M = 0.84 ± 0.20), Ago2-siVP1 (M = 0.42 ± 0.22), Ago2-siVP3 (M = 0.28 ± 0.05), Gw182-siIrr (M = 0.84 ± 0.20), GW182-siVP1 (M = 0.28 ± 0.02), Gw182-siVP3 (M = 0.26 ± 0.10), where M represents the percentage of NSP2 pixels (red) that overlap with GW182 or Ago2 pixels (green) (where M = 0 represent no colocalization and M = 1 represent 100% of colocalization).

in mock-infected cells, in which a discrete number of foci could be seen. A similar situation was observed in the case of Ago2, where the signal that appeared surrounding the viroplasms was not longer present in VP1- or VP3-silenced cells, and some of it appeared to be localized in fibers. These results suggest that the cellular distribution of these two proteins also depends on the concentration of viral RNA present in the cytoplasm of infected cells.

2.4. The cellular localization of HuR protein is also altered in rotavirus infected cells

Since our results suggested that several proteins that form part of RNA granules changed their localization in rotavirus-infected cells, we wanted to study if the cellular distribution of another RBP that does not typically form part of RNA granules was also altered due to infection. HuR is an RNA binding protein that is predominantly nuclear, but shuttles between the nucleus and the cytoplasm, and is known to influence the stability and translation of several cellular mRNAs (Abdelmohsen and Gorospe, 2010). We compared the localization of the HuR protein between mock-infected and infected cells by immunofluorescence microscopy. We found that while this protein is mostly present in the nucleus of mock-infected cells, it appears to accumulate in the cytoplasm of the cells infected with rotavirus (Fig. 5). Interestingly, when the amount of viral RNA was decreased in the cytoplasm, by silencing the expression of VP1, the nuclear localization of HuR was restored (Fig. 5). Taken together, these results suggest that

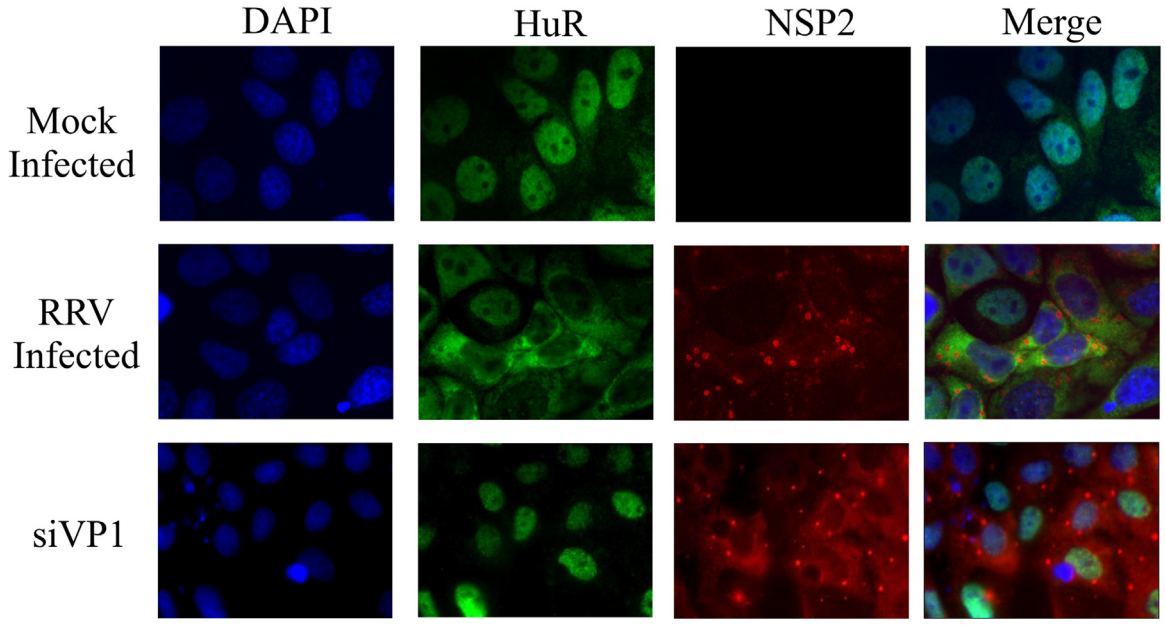

Fig. 5. The subcellular localization of HuR changes during rotavirus infection. MA104 cells grown in coverslips were either transfected with an siRNA to VP1 or mock-transfected and 72 h post-transfection cells were infected or not with RRV at an MOI of 5. Eight hpi cells were fixed and stained with antibodies against HuR (green), and to NSP2 (red), as indicated under Section 4. Cell nuclei were stained with DAPI (blue). The images were acquired in a Zeiss "Axioskop 2 mot plus" epifluorescence microscope.

during rotavirus infection, the amount of viral RNAs present in the cytoplasm seem to be modifying the distribution of several RBPs, preventing their usual cellular localization and probably their function.

2.5. Viral RNA binds to Xrn1, Dcp1, Ago2 and Hur in rotavirus-infected cells

To demonstrate a direct interaction between viral RNA and the proteins studied in this work we performed immunoprecipitation (IPP) assays of rotavirus-infected cell lysates, using mABs directed to Ago2, Xrn1, Dcp1 or HuR (the antibody against GW418 was not appropriate for IPP assays). As controls we used a mouse pre-immune antibody and two mABs against cellular proteins, the heat shock protein 70 or to protein phosphatase 1 (PP1), with no known RNA binding properties. The resulting IPPs were analyzed either by Western blot with the homologous antibodies to verify the immunoprecipitation (Fig. 6A), or were extracted with Trizol, and the presence of viral RNA was determined by end-point RT-PCR, using oligonucleotides that specifically amplify segment 10 mRNA (that encodes rotavirus NSP4) (Fig. 6B). We detected the presence of viral RNA segment 10 in the lysates that were immunoprecipitated with antibodies to Xrn1, Dcp1, Ago2, and HuR, but no viral RNA was detected when the lysates were immunoprecipitated with the control pre-immune mice antiserum or with the two control antibodies (anti-Hsp70 or anti-PP1). These results demonstrate that viral RNA interacts with the RBPs characterized in this work since it co-precipitated with antibodies against these proteins, and supports the idea that viral mRNA might be sponging cellular RBPs during the infection.

2.6. Role of the characterized RBPs during rotavirus infection

Since the cellular distribution of Xrn1, Dcp1, GW182, Ago2, and HuR was altered during rotavirus infection, we wonder whether these proteins had an anti-rotaviral activity and, thus, their trapping by viral RNA could be considered as a counter-measure to prevent their inhibitory function. To characterize the role of these proteins in the rotaviral cycle, we silenced their expression by RNAi and determined the amount of viral RNA that was made during the infection; we also quantitated the amount of mature infectious virus produced in the silenced cells. The effectiveness of each silencing was verified by western blot (Fig. 7A), and the effect of knocking down each of these proteins on the synthesis of viral RNA was determined by RT-qPCR, measuring the amount of the segment 10 mRNA. We found that when the expression of Dcp1 or GW182 was silenced, there was no change in the amount of viral RNA synthesized at 8 hpi, as compared to the amount synthesized in cells treated with an irrelevant siRNA. In contrast, when Ago2 and HuR were silenced, there was a decrease in the amount of NSP4 mRNA of about 50%. Interestingly, knocking down the expression of Xrn1 resulted in a two-fold increase in RNA synthesis, suggesting that even though the presence of this RNAse is reduced in PBs, it is still active degrading RNA (Fig. 7B), as has been previously reported (Decker et al., 2007). The effect of silencing these proteins on the replication cycle of rotavirus was measured by quantitating the amount of infectious virus produced in the absence of each RNA binding protein. Compared to the amount of virus produced in cells that were transfected with an irrelevant siRNA, we found that, as expected, when Xrn1 was silenced the amount of viral progeny increased about 4-fold. Silencing Dcp1 caused a two-fold increase, while knocking down the expression of GW182 did not affect the amount of infectious virus produced. When HuR was silenced, a reduction of about 50% in virus production was observed, in accordance to the reduction in viral RNA (Figs. 7B and 7C).

In contrast to these results, we found that when Ago2 was silenced there was a four-fold increase in viral progeny, while the amount of viral RNA detected under these conditions was decreased by 50% compared to the control transfected cells, suggesting that the viral RNA present in these cells might be more efficiently encapsidated. To test this idea, viral particles obtained from infected cells in which Ago2 was silenced, were partially purified by extracting the infected cell lysate with Freon and pelleting the viral particles through a 40% sucrose cushion. The amount of protein in the pellets was quantitated, and their infectivity was determined. In two independent experiments, we found that there were two times more infectious viral particles per μg of protein in cells in which Ago 2 was silenced compared to the particles obtained from cells treated with an irrelevant siRNA (Fig. 7D), suggesting that even though there was less viral RNA in Ago2 knocked down cells (Fig. 7B), it might be more efficiently encapsidated.

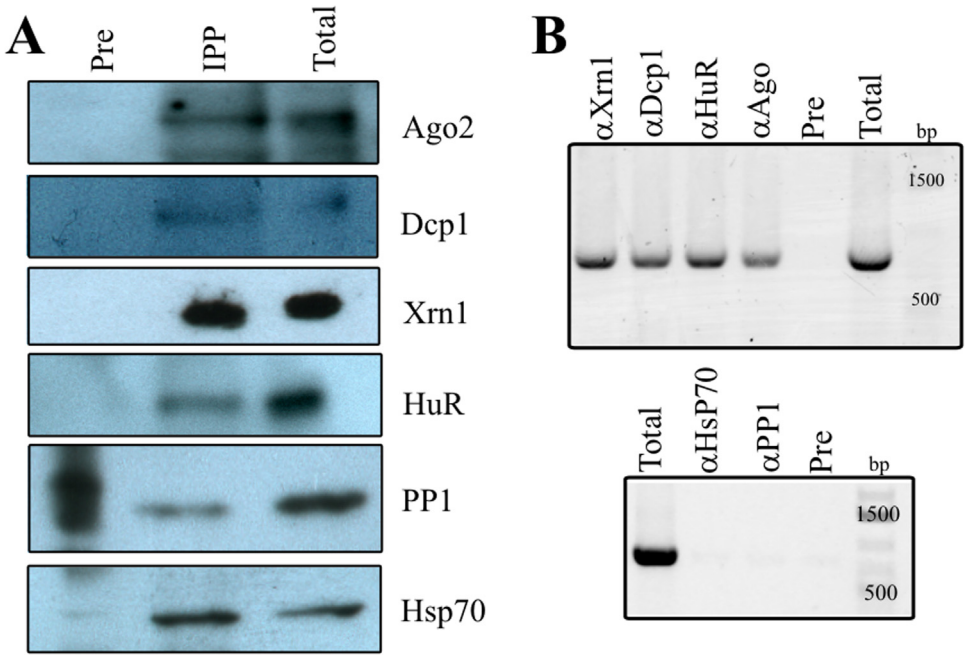

Fig. 6. Viral RNA binds to Xrn1, Dcp1, Ago2 and HuR in rotavirus-infected cells. Confluent MA104 cells grown in 150 mm^2 flasks were infected with RRV at an MOI of 5, and 8 hpi cells were sonicated and the cell lysate was immunoprecipitated (IPP) with the indicated mABs, or with a mouse pre-immune serum (Pre) as a control. A) The immunoprecipitates or a non-immunoprecipitated lysate (Total), were resolved in an SDS-10% PAGE, transferred to nitrocellulose and the indicated RBPs were detected by immunoblot analysis using the corresponding antibodies, or B) The RNA present in the IPPs or in a total lysate were extracted with Trizol, and RNA gene segment 10 of rotavirus was amplified by RT-PCR, and the products were resolved in 0.8% agarose gels as indicated under Materials and Methods.

3. Discussion

In this work, we have found that during rotavirus infection several RBPs change their distribution in the cell. The PBs present in the cytoplasm of infected cells, when stained with antibodies against two typical markers of these RNA granules, Xrn1 and Dcp1, appear to decrease in number, while the total amount of these two proteins does not change significantly. Looking for the distribution of GW182 and Ago2 proteins, which are known to be present in different RNA granules, we also found that their distribution was altered in the infected cells. A portion of GW182 seem to colocalize with viroplasms, while Ago2 was observed surrounding these viral structures. Furthermore, when the localization of an RBP that does not typically aggregates in RNA granules, HuR, was characterized, we found that it also changed its localization in infected cells, from being present mainly in the cell nucleus, to re-localize to the cell cytoplasm.

Interestingly all the changes in the subcellular localization of these proteins, could be reversed when the amount of viral RNA in rotavirus infected cells was reduced to about 10% the amount in control cells, through silencing the expression of either VP1, the viral RNA-polymerase, or VP3, a viral protein that besides having a methyl-guanyly transferase activity, contains a phosphodiesterase domain that cleaves the 2′-5′ oligoadenylates, preventing the activation of RNAse L (Sanchez-Tacuba et al., 2015). These observations suggest that the viral RNA could be interacting with the proteins characterized here, causing their re-localization.

Apparently, not all the interactions between the rotavirus transcripts and the cellular proteins are equal. In the case of the PBs proteins characterized here, their aggregation in RNA granules is clearly prevented. Bhowmick et al. (2015) made similar findings when characterizing the behavior of PBs in rotavirus infected cells, however, they found that Xrn1 and Dcp1 were relocalized to the nuclei of infected cells, as opposed to our findings that these proteins were no longer present in PBs, but rather were homogeneously dispersed in the cell cytoplasm. It is not easy to explain these different observations, however, we think that most of the differences noted between Bhowmick et al. and our work could be due to two main reasons. One is that the rotavirus strain that was mainly used in their work was the simian rotavirus strain SA11, which is different from the rhesus strain RRV we used in this work. Several different phenotypes have been noted when these two different rotavirus strains have been compared. For example, RRV and SA11 differ in their entry mechanism; while SA11 depends on clathrin-mediated endocytosis, RRV entry is clathrin- and caveolin-independent (Diaz-Salinas et al., 2014). Also, it was reported that the severity of disease and spread of rotavirus infection in mice differs depending on the virus strain used for inoculation, in this model RRV and SA11 showed different phenotypes (Ciarlet et al., 2002). The second, and most likely reason, could be that in the immunofluorescence assays shown in Bhowmick et al., the cells were treated with sodium arsenite, a well-known cellular stress inducer, and indeed it has been observed that this treatment could cause nuclear translocation of cytoplasmic proteins (see for example: (Garcia-Yague et al., 2013)). In our hands, during RRV infection we were not able to observe any nuclear translocation of Xrn1 or Dcp1. On the other hand, silencing the expression of these two proteins in rotavirus-infected cells had different phenotypes. While there was not a significant change in viral RNA or viral progeny produced in the absence of Dcp1, when Xrn1 was silenced both the amount of viral RNA transcripts and the infectious virus particles increased up to four-fold (in the case of viral progeny), suggesting that the activity of this cellular RNAse is deleterious for viral transcripts, and that even though during the infection is no longer present in PBs, it is still active.

In the case of GW-bodies, we found that during infection, a portion of GW182 clearly colocalized in viroplasms, however, the fact that knocking down the expression of this protein did not have a significant effect on the replication of rotavirus suggests that this interaction is not relevant for virus infection. In contrast, the interaction of Ago2 with viral RNA seem to have an impact during infection. A portion of this protein appeared surrounding the viroplasms, most probably interacting with the recently synthesized transcripts. When Ago2 was silenced, the amount of viral RNA decreased, but the total amount of infectious viral particles increased four-fold suggesting that the interaction of Ago2 with viral RNA might prevent its degradation, but also might be hampering its encapsidation into virions; indeed, we found that there were more infectious viral particles formed in Ago2 silenced cells (Fig. 7D); further experiments are needed to identify the mechanism by which Ago2 might be interfering with the encapsidation process.

We have previously shown that during the infection there is an enormous accumulation of viral RNA in the cytoplasm of infected cells;

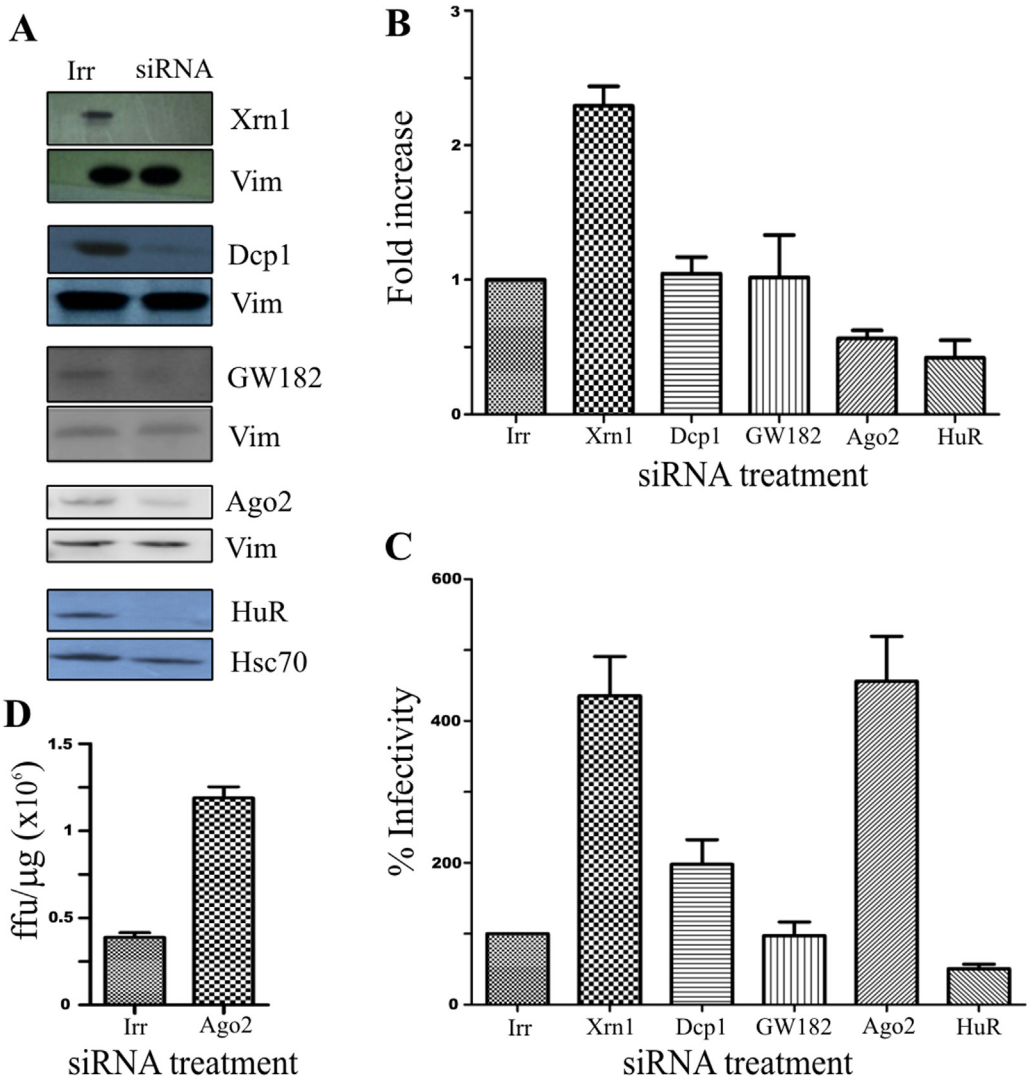

Fig. 7. Effect of the characterized RBPs in the replicative cycle of rotavirus. A) MA104 cells were transfected with the indicated siRNAs, and 72 h post-transfection were infected with RRV at an MOI of 5, and 8 hpi cells were lysed and the proteins were resolved in an SDS-10% PAGE, transferred to nitrocellulose and the indicated proteins were detected by immunoblot analysis using the indicated antibodies, anti-Vimentin (Vim), or anti Hsc70 (Hsc70) were used as loading controls. B) Total RNA was extracted from cell lysates with Trizol and the levels of rotavirus RNA gene segment 10, and 18S RNA were quantitated by RT-qPCR as indicated under Materials and Methods. The results were normalized to the levels of total 18S ribosomal RNA (rRNA18S) detected in each RNA sample. The RT-qPCR results are expressed as fold increase relative to the amount of gene 10 RNA present in infected cells that were transfected with the irrelevant control siRNA (Irr), which was taken as 1. The arithmetic means ± standard deviation of three independent experiments performed in triplicate are shown. C) In parallel wells, cells treated as in A) were harvested 15 hpi, lysed and the virus titer was determined by an immunoperoxidase focus forming assay as described under Materials and Methods. Data are expressed as the percentage of the infectivity obtained when the cells were transfected with an irrelevant siRNA (Irre), which was taken as 100% infectivity. The arithmetic means ± standard deviation of three independent experiments performed in duplicate are shown. D) Viral particles were semi-purified from rotavirus infected cell lysates that were transfected with an siRNA to Ago 2, or with siIRR, and their concentration and infectivity was determined as indicated under Materials and Methods. Data are expressed as focus forming units (ffu)/µg of protein. The arithmetic means ± standard deviation of two independent experiments performed in duplicate are shown.

by RT-qPCR we estimated that there are about 300,000 copies per cell of the RNA segment 10, and about 100,000 copies per cell of RNA segment 6 (Rubio et al., 2013). Considering that the rotavirus genome contains 11 RNA segments, a moderate calculation, thinking that there are about 100,000 copies of each segment, would give a rough estimate of 1.1×10^6 copies of viral mRNAs/cell, only about three times less than the amount of 18S rRNA per cell! Thus, it is highly likely that the amount of viral RNA present in the cell cytoplasm could sponge many of the RBPs of the cell changing their distribution and also altering their functions. The fact that decreasing 90% the amount of viral RNA present in the infected cells almost completely reverts the localization of these RBPs, suggests that this is the case. Indeed, viral mRNAs interact with Dcp1, Xrn1, Ago2, and HuR in rotavirus infected cells, since we found that viral RNA coprecipitated with these RBPs when immunoprecipitated with specific antibodies.

In general, the accumulation of large amounts of viral RNA in viral infections is not that uncommon and might be seen as a rudimentary measure used by viruses to ensure the efficient replication of their genome and the effective translation of their mRNAs to guarantee a successful infection. There is an increasing number of examples of viruses in which the accumulation of viral RNA in the cell's cytoplasm functions as a protein sponge, hijacking cellular RBPs proteins (Charley and Wilusz, 2014), with dengue virus and Sindbis virus being two well-known examples. In dengue virus infection, an accumulation of the small non-coding sfRNA takes place, the sfRNAs bind and down-regulate the activity of G3BP1, G3BP2, and CAPRIN1, inhibiting the response modulated by interferon β (IFN-β) (Bidet et al., 2014). In the case of Sindbis virus infection, there is a large accumulation of genomic and subgenomic RNAs in the infected cells that sequester HuR in the cytoplasm, preventing it from interacting with other cellular mRNAs. HuR is mainly present in the nuclei of cells, and its interaction with cellular transcripts prevents their degradation. The sponging of this protein in Sindbis virus infection most likely alters the regulation of cellular gene expression preventing the antiviral response of the cell (Barnhart et al., 2013). In addition, it has been recently shown that HuR specifically protects IFN-β mRNA from degradation (Herdy et al., 2015). Although we have not demonstrated that this is the case in rotavirus-infected cells, considering that most HuR seems to be sequestered by viral RNA in the cell cytoplasm, it is conceivable that this protein can no longer bind to and protect cellular mRNAs, causing their degradation; among these mRNAs could be the IFN-β mRNA and possibly several other genes of the innate immune response of the cell. Thus, it is tempting to propose that the sponging of cellular RBPs by rotavirus RNAs could be a strategy, not very refined, but effective

nonetheless, to suppress the antiviral responses of the host cell. None of the RBPs characterized in this work by itself seem to be able to significantly reduce the replication of rotavirus, but their activities might add-up to control viral replication. The sponging of these proteins by the huge amount of viral RNA that accumulates in the infected cell might be an effective, non-targeted viral response to control the action of these cellular RBPs.

4. Materials and methods

4.1. Cell culture and viruses

The rhesus monkey epithelial cell line MA104 (ATCC) was grown in Dulbecco's modified Eagle's medium (DMEM) reduced serum (Thermo Scientific HyClon, Logan, UT) supplemented with 5% heat-inactivated fetal bovine serum (FBS) (Biowest, Kansas, MO), at 37 °C in a 5% CO_2 atmosphere and was used for all experiments carried out in this work. The simian rotavirus strain RRV used in this work, was originally obtained from H. B. Greenberg (Standford University, Stanford, CA). The virus was propagated in MA104 cells as described previously (Pando et al., 2002). Prior to the infection, RRV was activated with trypsin (10 μg/ml, Gibco, Life Technologies, Carlsbad, CA) for 30 min at 37 °C.

4.2. Antibodies

Polyclonal antibodies to purified RRV TLPs and to vimentin were produced in rabbits as described previously (Lopez et al., 2005). Rabbit polyclonal sera to NSP2, has been described previously (Gonzalez et al., 1998). Monoclonal antibodies to Dcp1, Xrn1 and PPI were purchased from Santa Cruz Biotechnology (Santa Cruz, CA), GW182, and Ago2 were obtained from Abcam (Cambridge, MA) anti-HuR from Clonegene (Hartford, CT), anti-Hsc70 and anti Hsp70 from StressGen (San Diego, CA). Alexa Fluor 488- and 568-conjugated secondary antibodies were purchased from Invitrogen (Eugene, OR), horseradish peroxidase conjugated goat anti-rabbit polyclonal antibody was from KPL (Gaithersburg, MD), horseradish peroxidase-conjugated goat anti-mouse was from Millipore Merck KGaA (Darmstadt, Germany), and Dynabeads Protein G- LS10003D were from Thermo Scientific (Waltham, MA).

4.3. Infection of cells and titration of viral progeny

Cell monolayers in 24 or 48 wells plates were infected with an MOI of 5 and then incubated for 15 h. At this time cells were lysed by two freeze-thaw cycles, and the lysates were treated with 10 μg/ml of trypsin for 30 min at 37 °C. Infection titers of the viral preparation were obtained by an immunoperoxidase assay. Briefly, confluent cells in 96 wells plates were adsorbed with two-fold serial dilution of the above-mentioned viral lysate for 60 min at 37 °C. After adsortion, virus inoculum was removed, cells were washed once, fresh MEM was added, and the infection was left to proceed for 14 h for RRV at 37 °C. RRV-infected cells were detected by an immunoperoxidase focus detection assay using a rabbit hyperimmune serum to rotavirus, as described previously (Gutierrez et al., 2010). The numbers of focus-forming units (ffu's) were counted with Visiolab 1000 station (Biocom, France) as previously reported (Guerrero et al., 2000).

4.4. siRNA transfection

The small interfering RNAs (siRNAs) were purchased from GE Healthcare Dharmacon (Lafayette, CO). The sequence of the siRNAs against the rotavirus genes used in this work, have been previously reported (Montero et al., 2008). DCP1, Xrn1, Gw182, Ago2, HuR and the irrelevant control "NonTargeting" siRNAs were obtained from Dharmacon. Transfection of siRNAs into MA104 cells was performed in 48-well plates using a reverse transfection method as described previously (Gutierrez et al., 2010). Briefly, the siRNAs were transfected using Oligofectamine (Invitrogen. Eugene, OR), the transfection mixture was added to cells and kept for 12 h at 37 °C, after this time, the transfection mixture was replaced with MEM, and cells were incubated for 36 h at 37 °C prior to virus infection.

4.5. Semi-purification of viral particles

MA104 cells grown in six well plates were transfected with siRNAs as previously mentioned, and 72 h post-transfection were infected with RRV at an MOI of 5. Twelve hpi cells were harvested by scraping in TNC buffer (10 mM Tris-HCl [pH7.5], 140 mM NaCl, 10 mM $CaCl_2$), sonicated 3 times for 20 s on ice, and centrifuged at 1000 rpm for 5 min to remove cell debris. The supernatant was then extracted with Freon, and the aqueous phase was layered on top of a 2 ml 40% sucrose cushion and centrifuged for 2 h at 40,000 rpm at 4 °C in an SW40 rotor. The pellet containing the viral particles was resuspended in 100μl of TNC buffer, quantified by Nanodrop and used for infectivity assays as previously described.

4.6. Immunofluorescence

MA104 cells grown on glass coverslips were transfected or mock transfected and infected or mock-infected as indicated in the Figure Legends. At 4, 6 or 8 h post-infection (hpi), cells were fixed with 2% paraformaldehyde in PBS for 20 min at room temperature and the coverslips were washed twice with washing buffer (PBS with 50 mM ammonium chloride). Fixed cells were permeabilized by incubation in 0.5% Triton X-100 in PBS with 50 mM ammonium chloride for 15 min at room temperature, and then were blocked by incubation with 1% bovine serum albumin (BSA), 50 mM NH_4Cl in PBS at room temperature for 1 h. The coverslips were incubated for 1 h with primary antibodies diluted in blocking buffer (PBS, 50 mM NH4Cl, 1% BSA) at room temperature, and washed three times in washing buffer. The cells were incubated with the secondary antibody in blocking buffer for 1 h at room temperature, washed 3 times and incubated with 30 nm 4′,6-Diamidino-2-phenylindole dihydrochloride (DAPI) (Invitrogen, Eugene, OR) for 30 min, and finally washed 4 times with washing buffer and mounted on glass slides with Citifluor AF1 (Emsdiasum, Hatfield Penn). The slides were analyzed with a Zeiss "Axioskop 2 mot plus" epifluorescence microscope coupled to a photometrics CoolSNAP HQ2 CCD camera. For confocal images we use an Olympus confocal FluoView 1000 multifotonic or a 3I Marianas spinning disk confocal microscope. The quantitative colocalization analysis of NSP2 with GW182 and Ago2 was performed using stacks of confocal images analyzed with the plugin "Coloc 2" of the Fiji-imageJ software, to determine Manders'(M) colocalization coefficient (Costes et al., 2004; Manders et al., 1993).

4.7. End point RT-PCR analysis of RNA segment 10

Total RNA was isolated from protein G immunoprecipitates, or from total non- precipitated cell lysate using TrIzol reagent (Invitrogen, Carlsbad, CA) as indicated by the manufacturer. cDNA was reverse transcribed from 1 μg of total RNA using the M-MuLV reverse transcriptase (NEBioLabs) and amplified with Vent polymerase (NEBioLabs) using the following primers: YM10-5′: CAGACCCGGGTACCTTTTAAA AGTTCTGTTCC and YM10-3′: CAGACCCGGGCCGCGGTCACATTAAGA CCGTTC; the amplified fragment of ~700 bp corresponding to gene segment 10, was separated in 0.8% TAE-agarose gels, visualized by ethidium bromide staining, and detected using a Typhoon FLA9500 (GE).

4.8. Real time RT-PCR analysis

Confluent MA104 cells in 48-well plates were infected with RRV and harvested at different time points with Trizol. Total RNA was purified

and treated with RNA-free DNase (Roche, Basel, Switzerland) to eliminate possible DNA contamination. The primers used for the amplification of rotavirus RNA segment 10 have been described previously (Ayala-Breton et al., 2009). To determine the levels of the positive RNA strand, RT-qPCR was performed separating the reverse transcription and the PCR steps, as described by Ayala-Breton et al. (2009). Quantitative analysis of data was performed using Prism 7000 analysis software (Applied Biosystems, Life Technologies, Carlsbad, CA). The results were normalized to the levels of total 18S ribosomal RNA (rRNA18S) detected in each RNA sample. The changes in gene expression were calculated by the $2^{-\Delta\Delta CT}$ method, where *CT* is the threshold cycle (Livak and Schmittgen, 2001). The sequence of the rRNA 18S primers used in these assays were: rRNA18sfw: CGAAAGC ATTTGCCAAGAAT, and rRNA18srv: GCATCGTTTATGGTCGGAAC

4.9. Immunoblot analysis

Cells were lysed in Laemmli sample buffer and denatured by boiling for 5 min. Proteins in cell lysates were separated in SDS-10% PAGE and transferred to Immobilon NC (Millipore, Merck KGaA, Darmstadt) membranes. The membranes were blocked by incubation with 5% nonfat dry milk in phosphate-buffered saline (PBS) for 1 h at room temperature, and with primary antibodies diluted in PBS containing 5% milk, followed by an incubation with secondary, species-specific, horseradish peroxidase-conjugated antibodies, as previously reported (Gutierrez et al., 2010). The peroxidase activity was developed using the Western Lightning Chemiluminescence Reagent Plus (Perkin Elmer Life Sciences, Boston, MA), following the manufacturer's instructions. The blots were also probed with an anti-vimentin antibody, which was used as a loading control. Finally, the quantification analysis was performed using ImageJ software.

4.10. Immunoprecipitation assays

Confluent MA104 cells grown in 150 mm^2 flasks were infected with RRV at an MOI of 5, and 8 hpi cells were washed with PBS, scraped, collected and sonicated 4 times for 5 s at 4 °C; the cell extract was centrifuged at 1000 rpm for 5 min at 4 °C and the supernatant was collected. 1 ml of the cell lysate were precleared by incubation with 100 µl of protein-G magnetic beads at 4 °C for 1 h. The precleared supernatants were incubated with 1–5 µg of the indicated mABs for 1 h at 4 °C with agitation, a fresh suspension of protein G beads was added and incubated 2 h at 4 °C with agitation. After this time the beads were washed 3 times with RIPA Buffer (1% Triton X-100, 1% deoxycholic acid, 50 mM Tris-HCl [pH 7.5], 150 mM NaCl, 0.1% SDS) and finally the magnetic beads were divided in two tubes, one was resuspended in Laemmli Buffer, and denatured by boiling for 5 min. Proteins in the immunoprecipitates were separated in SDS-10% PAGE and transferred to Immobilon NC (Millipore, Merck KGaA, Darmstadt) membranes and analyzed by immunoblot using the same antibodies that were used for the IPP assay. The remaining tube of each IPP was extracted with Trizol and subjected to RT-PCR.

Acknowledgements

We are grateful to Rafaela Espinosa, and Marco Antonio Espinoza for their excellent technical assistance, and to Roberto P. Rodriguez-Bahena for software support. The services of the Laboratorio Nacional de Microscopía Avanzada (LNMA) funded by CONACyT are deeply recognized.

Funding

This work was supported by Grants IG200317 from Dirección General de Asuntos del Personal Académico, Universidad Nacional Autónoma de México, and 153639 from Consejo Nacional de Ciencia y Tecnología. AO was a recipient of a scholarship from CONACYT.

References

Abdelmohsen, K., Gorospe, M., 2010. Posttranscriptional regulation of cancer traits by HuR. Wiley Interdiscip. Rev. RNA 1, 214–229.
Anderson, P., Kedersha, N., 2008. Stress granules: the Tao of RNA triage. Trends Biochem. Sci. 33, 141–150.
Ayala-Breton, C., Arias, M., Espinosa, R., Romero, P., Arias, C.F., Lopez, S., 2009. Analysis of the kinetics of transcription and replication of the rotavirus genome by RNA interference. J. Virol. 83, 8819–8831.
Barnhart, M.D., Moon, S.L., Emch, A.W., Wilusz, C.J., Wilusz, J., 2013. Changes in cellular mRNA stability, splicing, and polyadenylation through HuR protein sequestration by a cytoplasmic RNA virus. Cell Rep. 5, 909–917.
Bhowmick, R., Mukherjee, A., Patra, U., Chawla-Sarkar, M., 2015. Rotavirus disrupts cytoplasmic P bodies during infection. Virus Res. 210, 344–354.
Bidet, K., Dadlani, D., Garcia-Blanco, M.A., 2014. G3BP1, G3BP2 and CAPRIN1 are required for translation of interferon stimulated mRNAs and are targeted by a dengue virus non-coding RNA. PLoS Pathog. 10, e1004242.
Charley, P.A., Wilusz, J., 2014. Sponging of cellular proteins by viral RNAs. Curr. Opin. Virol. 9, 14–18.
Ciarlet, M., Conner, M.E., Finegold, M.J., Estes, M.K., 2002. Group A rotavirus infection and age-dependent diarrheal disease in rats: a new animal model to study the pathophysiology of rotavirus infection. J. Virol. 76, 41–57.
Costes, S.V., Daelemans, D., Cho, E.H., Dobbin, Z., Pavlakis, G., Lockett, S., 2004. Automatic and quantitative measurement of protein-protein colocalization in live cells. Biophys. J. 86, 3993–4003.
Crawford, S.E., Ramani, S., Tate, J.E., Parashar, U.D., Svensson, L., Hagbom, M., Franco, M.A., Greenberg, H.B., O'Ryan, M., Kang, G., Desselberger, U., Estes, M.K., 2017. Rotavirus infection. Nat. Rev. Dis. Prim. 3, 17083.
Decker, C.J., Teixeira, D., Parker, R., 2007. Edc3p and a glutamine/asparagine-rich domain of Lsm4p function in processing body assembly in Saccharomyces cerevisiae. J. Cell Biol. 179, 437–449.
Diaz-Salinas, M.A., Silva-Ayala, D., Lopez, S., Arias, C.F., 2014. Rotaviruses reach late endosomes and require the cation-dependent mannose-6-phosphate receptor and the activity of cathepsin proteases to enter the cell. J. Virol. 88, 4389–4402.
Estes, M.Ka.G., H.D., 2013. Rotaviruses and their replication. In: Knipe, D.N., Howley, P.M. (Eds.), Field's Virology, 6th ed. Wolters Kluwer, Lippincott Williams & Wilkins, Philadelphia, PA., pp. 1347–1401.
Garcia-Yague, A.J., Rada, P., Rojo, A.I., Lastres-Becker, I., Cuadrado, A., 2013. Nuclear import and export signals control the subcellular localization of Nurr1 protein in response to oxidative stress. J. Biol. Chem. 288, 5506–5517.
Gonzalez, R.A., Torres-Vega, M.A., Lopez, S., Arias, C.F., 1998. In vivo interactions among rotavirus nonstructural proteins. Arch. Virol. 143, 981–996.
Guerrero, C.A., Zarate, S., Corkidi, G., Lopez, S., Arias, C.F., 2000. Biochemical characterization of rotavirus receptors in MA104 cells. J. Virol. 74, 9362–9371.
Gutierrez, M., Isa, P., Sanchez-San Martin, C., Perez-Vargas, J., Espinosa, R., Arias, C.F., Lopez, S., 2010. Different rotavirus strains enter MA104 cells through different endocytic pathways: the role of clathrin-mediated endocytosis. J. Virol. 84, 9161–9169.
Herdy, B., Karonitsch, T., Vladimer, G.I., Tan, C.S., Stukalov, A., Trefzer, C., Bigenzahn, J.W., Theil, T., Holinka, J., Kiener, H.P., Colinge, J., Bennett, K.L., Superti-Furga, G., 2015. The RNA-binding protein HuR/ELAVL1 regulates IFN-beta mRNA abundance and the type I IFN response. Eur. J. Immunol. 45, 1500–1511.
Livak, K.J., Schmittgen, T.D., 2001. Analysis of relative gene expression data using real-time quantitative PCR and the 2(-Delta Delta C(T)) Method. Methods 25, 402–408.
Lopez, T., Camacho, M., Zayas, M., Najera, R., Sanchez, R., Arias, C.F., Lopez, S., 2005. Silencing the morphogenesis of rotavirus. J. Virol. 79, 184–192.
Manders, E.M.M., Verbeek, F.J., Aten, J.A., 1993. Measurement of co-localization of objects in dual-colour confocal images. J. Microsc. 169, 375–382.
Montero, H., Arias, C.F., Lopez, S., 2006. Rotavirus nonstructural protein NSP3 is not required for viral protein synthesis. J. Virol. 80, 9031–9038.
Montero, H., Rojas, M., Arias, C.F., Lopez, S., 2008. Rotavirus infection induces the phosphorylation of eIF2alpha but prevents the formation of stress granules. J. Virol. 82, 1496–1504.
Moon, S.L., Wilusz, J., 2013. Cytoplasmic viruses: rage against the (cellular RNA decay) machine. PLoS Pathog. 9, e1003762.
Pando, V., Isa, P., Arias, C.F., Lopez, S., 2002. Influence of calcium on the early steps of rotavirus infection. Virology 295, 190–200.
Patel, P.H., Barbee, S.A., Blankenship, J.T., 2016. GW-bodies and P-bodies constitute two separate pools of sequestered non-translating RNAs. PLoS One 11, e0150291.
Poblete-Duran, N., Prades-Perez, Y., Vera-Otarola, J., Soto-Rifo, R., Valiente-Echeverria, F., 2016. Who regulates whom? An overview of RNA granules and viral infections. Viruses 8.
Rubio, R.M., Mora, S.I., Romero, P., Arias, C.F., Lopez, S., 2013. Rotavirus prevents the expression of host responses by blocking the nucleocytoplasmic transport of polyadenylated mRNAs. J. Virol. 87, 6336–6345.
Sanchez-Tacuba, L., Rojas, M., Arias, C.F., Lopez, S., 2015. Rotavirus controls activation of the 2'-5'-oligoadenylate synthetase/RNase L pathway using at least two distinct mechanisms. J. Virol. 89, 12145–12153.
Tsai, W.C., Lloyd, R.E., 2014. Cytoplasmic RNA granules and viral infection. Annu. Rev. Virol. 1, 147–170.